Autofluorescence Distribution Associated with Drusen in Age-Related Macular Degeneration

François C. Delori,[1,2] *Mark R. Fleckner,*[1] *Douglas G. Goger,*[1] *John J. Weiter,*[1,2] *and C. Kathleen Dorey*[1,2]

Purpose. To determine whether drusen in patients with age-related maculopathy and macular degeneration (ARM/AMD) are associated with focal changes in retinal pigment epithelium (RPE) lipofuscin fluorescence.

Methods. A new autofluorescence imaging device was used to study lipofuscin distribution associated with individual drusen in 20 patients with ARM/AMD. Paired monochromatic and autofluorescence fundus images were used for detailed analysis of the topography of autofluorescence at specific sites containing drusen. In four eyes, image analysis was used to compare the spatial distribution of the autofluorescence with the location of drusen and to quantify the autofluorescence distribution over individual drusen (54 drusen).

Results. A specific pattern of autofluorescence was frequently found to be spatially associated with hard drusen and soft drusen between 60 and 175 μm in size. The pattern is characterized by a central area of decreased autofluorescence surrounded, in most cases, by an annulus of increased autofluorescence. The location of this pattern was highly correlated with the position of individual distinct drusen. The central low autofluorescence focus was on average 16% below the surrounding background, and the annulus, when present, was on average 6% more fluorescent than the background. Soft drusen larger than 175 μm and confluent soft drusen show either multifocal areas of low autofluorescence or a more heterogeneous distribution.

Conclusions. Autofluorescence imaging permits measurement of RPE lipofuscin at specific sites. RPE overlying drusen have altered autofluorescence, suggesting changes in RPE health. (*Invest Ophthalmol Vis Sci.* 2000;41:496–504)

The first sign of impending pathology in age-related macular degeneration (AMD) is the appearance of retinal pigment epithelium (RPE) mottling and soft drusen, whitish spots with indistinct edges in the fundus. Soft drusen are recognized histologically as a localized thickening of Bruch's membrane, and the ultrastructure of these thickened areas demonstrate an accumulation of membranous debris in the inner collagenous layer of Bruch's membrane (basal linear deposits).[1–5] Their location and the composition of the lipids[6] are consistent with their derivation from RPE and photoreceptor membranes. Hard drusen, that occur in both AMD and normal aging, are discrete hyaline deposits that bulge inward, lifting the RPE and its basement membrane.[3–5]

The aging RPE is characterized by massive accumulation of lipofuscin,[7–9] which contains several fluorophores.[10] The predominant, deep orange fluorophore was determined to be an adduct of two vitamin A molecules and ethanolamine (A2-E).[11] When fed to cultured RPE cells, A2-E inhibits lysosomal degradation of proteins.[12] Thus, incomplete digestion of photoreceptor membranes could account for their accumulation in Bruch's membrane in the formation of drusen.

Lipofuscin fluorescence can be studied noninvasively by spectrophotometry[13–17] and/or imaging.[18–23] Spectral studies[13,15] of fundus autofluorescence (AF) have demonstrated that it exhibits the spatial distribution, excitation (Ex) and emission (Em) spectra, age-related increases, and localization among retinal layers that are characteristic of RPE lipofuscin.[7,9,10] Observations in patients with AMD suggest that elevated lipofuscin may precede or coexist with the earliest stages of pathology in age-related maculopathy (ARM) but that advanced stages of pathology are associated with decreased RPE lipofuscin.[14,16] Spectral measurements in fundus regions containing many drusen have demonstrated a shift of the emission spectrum toward short wave lengths, suggesting a contribution from drusen fluorophores.[14,17] Furthermore, because RPE over drusen in histologic sections can appear stretched and thin, it was reasonable to question whether drusen would be associated with alterations in the distribution of lipofuscin in the overlying RPE.

Imaging of fundus AF, using the scanning laser ophthalmoscope (SLO),[18] has made it possible to correlate changes in AF distribution with pathologic features.[18–23] In AMD patients, AF imaging has shown that AF is very low in areas of atrophy, high in the junctional zone around areas of atrophy,[19,23] and increased in focal areas of hyperpigmentation.[20] However, no consistent conclusions have been drawn about the AF levels over drusen,[20,22] and there have been no reports on a specific spatial AF distribution over individual drusen. In fact, drusen

From the [1]Schepens Eye Research Institute, and [2]Harvard Medical School, Boston, Massachusetts.

Supported by National Institutes of Health Grant EY8511 and a grant from the Massachusetts Lions Eye Research Fund, Inc.

Submitted for publication May 27, 1999; revised August 27, 1999; accepted September 13, 1999.

Commercial relationships policy: N.

Corresponding author: François C. Delori, Schepens Eye Research Institute, 20 Staniford Street, Boston, MA 02114.
delori@vision.eri.harvard.edu

Investigative Ophthalmology & Visual Science, February 2000, Vol. 41, No. 2

are often not individually recognized in SLO autofluorescence images.

We investigated RPE lipofuscin distribution in ARM/AMD using a non-SLO imaging device. We found a variety of AF distributions in the RPE over and around drusen, related to the presence of drusen but not associated with specific drusen. However, we found that a distinct AF pattern was frequently associated with hard drusen and soft drusen. This pattern, which is spatially associated with individual drusen, consists of a center with low AF, surrounded, in some cases, by an annulus of high AF.[24]

METHODS

Subjects

We obtained AF images in 19 patients with ARM/AMD (ages, 52–80 years) and 12 subjects with small hard drusen (<60 μm) but no clinically observed ARM (ages, 40–79 years).[25] All patients were referred from local ophthalmic practices and had complete clinical data, including color photographs and angiograms. Drusen sizes were measured on magnified color transparencies using an overlay containing standard sizes.[25] The pupil of one eye was dilated to a diameter of at least 6.5 mm. The tenets of the Declaration of Helsinki were followed, Institutional Review Board approval was granted, and informed consent was obtained for all subjects.

AF Imaging

AF images were obtained with a modified Topcon fundus camera (TRC-FE; Topcon Corp., Tokyo, Japan) coupled to a scientific grade CCD camera operated at −20°C (MicroMax; RS Princeton Instruments, Trenton, NJ). An aperture, inserted in the illumination optics of the camera, restricted the field of fundus excitation to a 13° diameter circle (to minimize the loss in contrast caused of light scattering and fluorescence from the crystalline lens). Two filter combination were used for AF imaging: a 470-nm excitation filter [central wavelength, 467 nm; full width at half maximum or minimum (FWHM), 30 nm] with a high-pass OG515 blocking filter (1% of maximum transmission at 499 nm; half maximum at 513 nm); and a 550-nm excitation filter (central wavelength, 548 nm; FWHM, 27 nm) with a high-pass OG590 blocking filter (1% maximum at 576 nm; half maximum at 587 nm). Excitation filters were of the interference type (Omega Optical, Brattleboro, VT), whereas the blocking filters were 6-mm-thick glass absorbing filters (Schott Glass Technologies, Duryea, PA). The rejection of each filter combination was higher than 10,000 at all wavelengths. A lens located between the fundus camera optics and the CCD array imaged the 13° diameter retinal field into a 4.5-mm-diameter circle within the rectangular array (6.9 × 4.6 mm, 768 × 512 pixels; 9 μm square pixels). The overall retina CCD magnification was then 1.16 mm/mm (instead of 2.42 mm/mm for the standard camera, which represents a light gain of 4.4). Images were recorded with 4 CCD pixels grouped into one. The size of this combined pixel was then 2 × (9 μm)/1.16 = 15.6 μm at the retina (we will be refer to this area as 1 pixel).

After alignment of the subject's pupil to the camera, retinal focus was attained by observing the CCD monitor (200-msec exposures, every 0.6 seconds) under illumination with the 550-nm filter. A 550-nm monochromatic image[26] was obtained with the 50 W/sec xenon flash setting. AF images (Ex = 470 nm, Em > 515 nm and Ex = 550 nm, Em > 590 nm) were obtained using the 300-W/sec setting. Retinal exposure for AF imaging was 3 to 5 mJ/cm^2 (flash duration, 1–2 msec), which is more than 1000 times lower than maximum permissible light levels.[27] Acquired images were transferred using 12 bit conversion (gray levels, 0–4095) into a computer, under control of IPLab Spectrum software (Scanalytics, Fairfax, VA). Gray levels were typically 300 to 1300 (above CCD black level) for monochromatic images, 30 to 180 for AF images with Ex = 470 nm, and 50 to 200 for AF images with Ex = 550 nm.

Image Analysis

Quantitative measurements of AF and reflectance over drusen were made using IGOR image analysis software (WaveMetrics, Lake Oswego, OR). After subtracting the CCD black level, monochromatic images were aligned to AF images using translations and matching the position of retinal landmarks in the superimposed images. Variations in the background (low spatial frequencies) were eliminated by creating a heavily smoothed copy of the original image using convolution with a Gaussian filter (half-width, 50–60 pixels, approximately $\frac{1}{4}$ of the field diameter) and by dividing the original image by the smoothed image. The resulting "flattened" image has minimal background variation, with no significant change in the signal distribution at small individual features. The mean level in the flattened images was ~1, and the SD was typically 0.08 to 0.15 (compared to 0.2–0.4 in the original image).

Spatial correspondence of the foci of low AF with drusen was investigated as follows. Thresholding in the flattened monochromatic images was used to identify pixels clearly associated with drusen and those associated with vessels. "Drusen" pixels had reflectance greater than background by at least $^1/_2$ SD. "Vessel" pixels were identified as those with reflectance more than 20% below background. In the flattened AF images, "low AF" pixels were defined as having an AF below background by at least $\frac{1}{2}$ SD. All pixels associated with vessels were removed from both images. The resulting binary images were superimposed, allowing to obtain counts (a, b, c, d) of four types of pixels: (a) pixels with "low AF" and associated with a "druse," (b) pixels with no "low AF" but associated within a "druse," (c) pixels with "low AF" but not corresponding with a "druse," and (d) pixels containing neither "low AF" nor "drusen." The total number of pixels is then $N = a + b + c + d$. The probability of a low AF pixel to occur on a druse a/N was compared to the predicted probability of the same event occurring with randomly distributed drusen and low AF pixels $(a + b)(a + c)/N^2$. The comparison was assessed with *Z*-test statistics assuming binomial distribution.

The autofluorescence and reflectance distributions at individual drusen were determined by first locating crosshairs at the center of the druse and at the center of the focus of low AF. Average signals $S(r)$ in concentric annuli (1 pixel wide) with center radii $r = 0, 1, 2, \ldots$, and 12 pixels were then computed (1 pixel: 15.6 μm at the retina). To avoid neighboring features (such as vessels or other drusen), the operator could perform this averaging in a segment (e.g., signals were averaged clockwise between 3 and 9 o'clock to avoid a horizontal vessel located above the druse). With the $S(r)$ profiles displayed, the operator selected—aided by plots of the differentials of each profile—the annulus (radius = r_b), where *both* profiles started to flatten outside the druse. The average backgrounds $S(r_b)$ were computed in a 3-pixel-thick (46.8 μm) background annu-

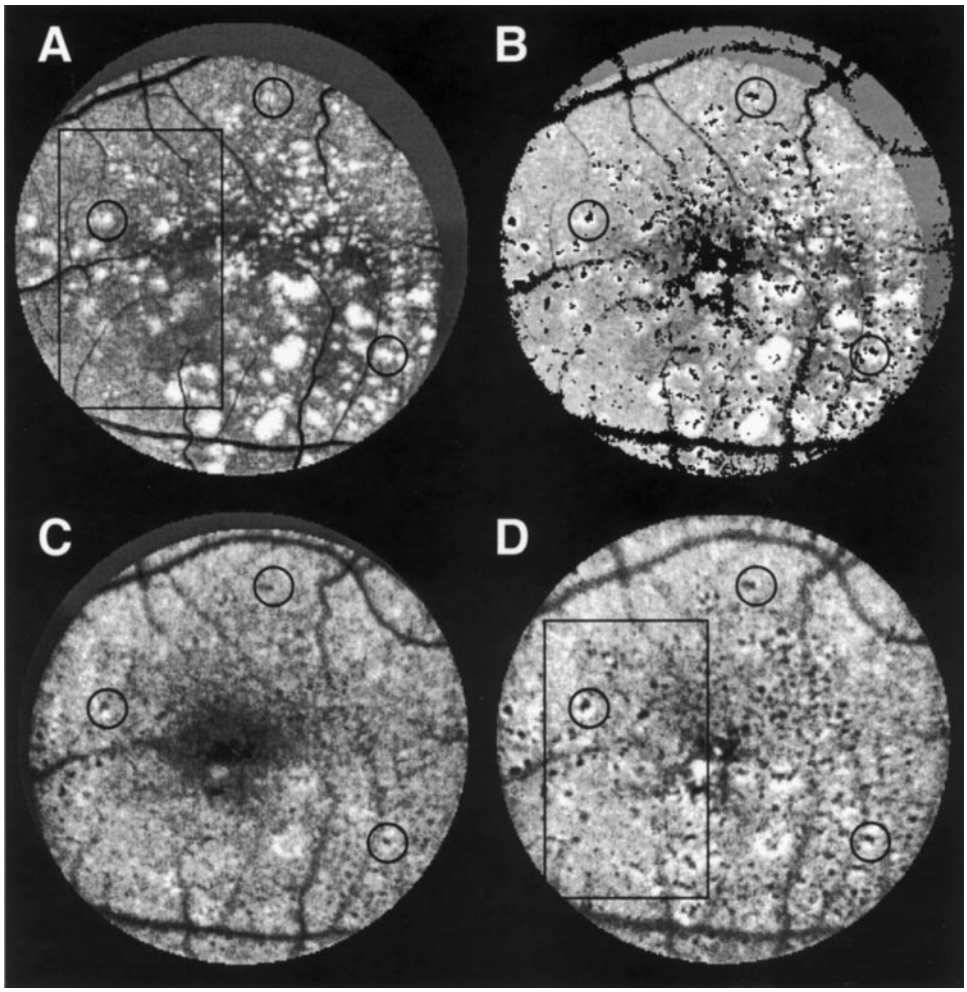

FIGURE 1. Monochromatic and autofluorescence images in the left eye of a 70-year-old man (patient 1) with hard and large soft drusen secondary to AMD [visual acuity (VA), 20/25]. The monochromatic image (**A**) was obtained with 550-nm illumination. (**C**, **D**) The AF images were obtained with Ex 470 nm (Em > 515 nm) and Ex 550 nm (Em > 590 nm), respectively. The field is approximately 13° in diameter. All images were aligned to the image in (**D**). *Circles* around drusen serve as guide for comparison of the images. The *rectangle* indicates where quantitative analysis of individual drusen was performed. In the composite image (**B**) the dark foci from the AF image (binary image showing pixels < 85% of the mean) have been superimposed on the monochromatic image.

lus with r_b as inner radius. The profiles were expressed as the relative deviation from the average backgrounds $S(r_b)$ by

$$P(r) = \frac{S(r) - S(r_b)}{S(r_b)}. \quad (1)$$

Positive (negative) values of $P(r)$ indicate signal levels higher (lower) than the background. The FWHM and the center value $P(0)$ for all AF and reflectance profiles were calculated, as well as the diameter and amplitude of the AF annulus. To evaluate the effect of a systematic change of the selected inner radius of the background averaging annulus r_b, we recalculated all parameters presented in the results, using (r_b + 15.6 μm) or (r_b −15.6 μm) instead of r_b. When moving the annulus toward the center of the druse (r_b − 15.6 μm), significant but small changes were observed: for the reflectance (AF) profiles, the FWHM changed on average by −1.6% (+1.9%) and the central $P(0)$ by −4.2% (+5.0%); for the AF profile the amplitude of the ring of high AF changed by −20%, but the diameter of that ring was not affected. All changes were smaller when the background annulus was moved away from the center (r_b + 15.6 μm). Correlations determined in this study as well as subdivision of drusen profiles in different types were not substantially affected by either change in position of the background integration area.

RESULTS

AF and monochromatic reflectance images of four patients with soft and hard drusen are presented in Figures 1 to 3. Information about the individual patients are given in the legends. Green monochromatic images inherently have higher contrast than color transparencies, which permits the detection of smaller drusen and creates sharp boundaries around soft and confluent drusen. All images were aligned with each other, and background variations were minimized.

AF Distribution Pattern over Drusen

The monochromatic image of patient 1 (Fig. 1A) shows numerous soft and hard drusen. The AF images (Figs. 1C, 1D) exhibited numerous foci where fluorescence was lower than background. Most of these dark foci were surrounded by a marked annulus of fluorescence above background, creating a torus pattern (type A pattern). Alternatively, some low AF foci are not surrounded by an annulus (type B pattern). In the composite image (Fig. 1B) most, but not all, of the drusen have distinct low AF foci near their center. Comparison of AF images using 470- and 550-nm excitation (Figs. 1C, 1D) indicates that the latter afforded greater contrast between the AF patterns and the background, although the contrast of vessels was lower. Moreover, foveal details in the 470-nm image (Fig. 1C) were

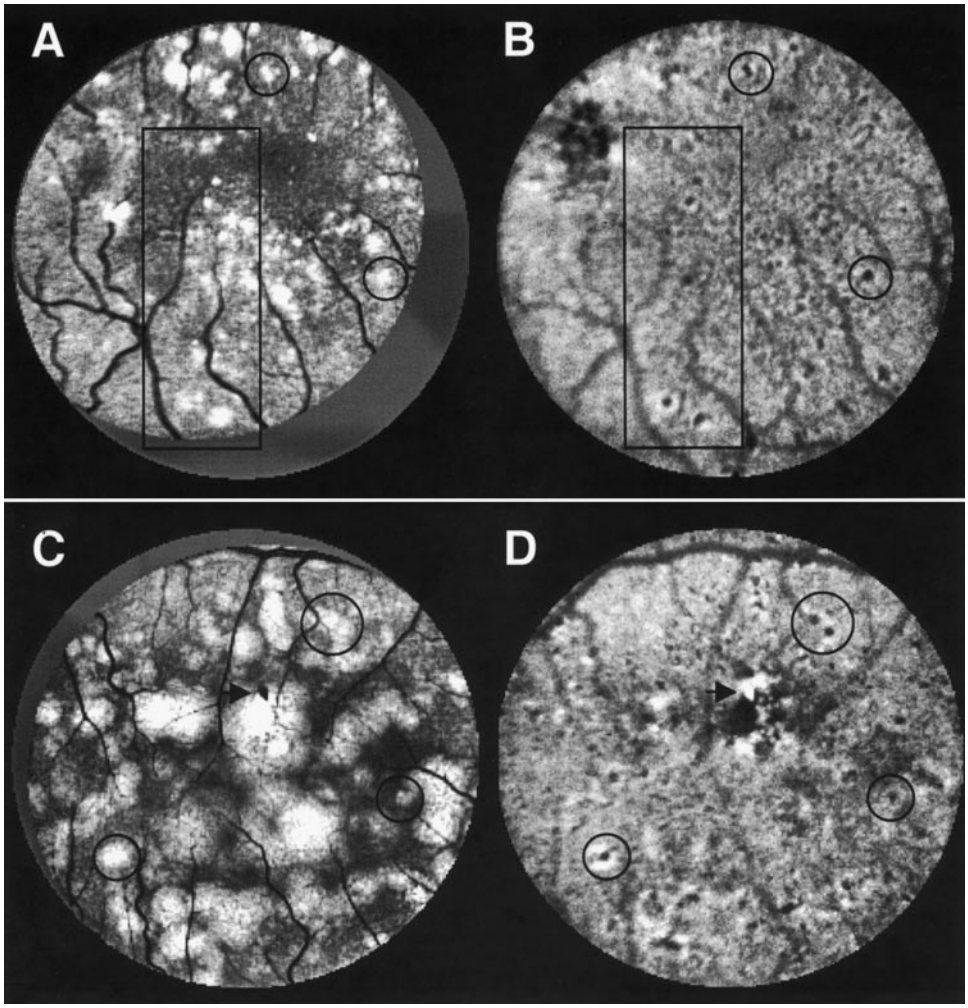

FIGURE 2. Monochromatic (**A** and **C**; 550 nm) and autofluorescence (**C**, **D**; Ex 550 nm, Em > 590 nm) images in two patients with AMD. (**A**, **B**) Patient 2 was a 69-year-old man with hard and soft drusen (right eye; VA, 20/25). (**C**, **D**) Patient 3 was a 70-year-old man with diffuse large and confluent soft drusen in the macula (right eye; VA, 20/40). The monochromatic images were aligned with the AF images. *Circles* around drusen serve as guide for comparison of the images. Quantitative analysis of drusen was performed in the area enclosed by a *rectangle* for patient 2, and in the entire field for patient 3. Note an area of partial atrophy at the *top left corner* of the rectangle in patient 2 (**B**) and in patient 3 (**C**, **D**) a small area of hyperpigmentation (*arrows*) that appears dark under monochromatic light, but is highly fluorescent in the AF image.

obscured by the absorption of the macular pigment, but this was not the case in the 550-nm AF image (Fig. 1D).

The drusen-associated patterns of AF were also observed in patients 2 and 3 (Fig. 2). In patient 2 (Figs. 2A, 2B), very distinct AF patterns associated with soft drusen are observed (see bottom of image, in rectangle), as well as an area with multiple large foci of decreased AF that are not spatially correlated with individual drusen in the monochromatic image (upper left corner of rectangle). We interpret this decreased AF as representing RPE thinning and early atrophy. In patient 3 (Figs. 2C, 2D), drusen larger than 175 μm were found to have less consistent patterns, whereas confluent drusen have multifocal areas of low AF. The latter appear to mark the sites of adjacent individual drusen that became confluent over time and lost their individual borders.

Small hard drusen (<60 μm), frequently observed in the aging eye, are not associated with a clear AF pattern. Although it was possible to see correspondence between localized low- or high-AF sites with the position of hard drusen, the majority of the individual foci were very small (containing 4 pixels or less, <30-μm diameter) and possibly below the resolution of the technique. However, AF patterns are seen overlying larger (>60 μm) hard drusen in AMD eyes (Figs. 1, 2). Numerous AF patterns also are observed in patient 4 (Fig. 3), who has a large number hard and soft drusen (40–150 μm), but it is difficult to visually ascertain the concordance of the AF patterns and drusen.

Additional images of 15 patients with AMD/ARM were analyzed. Hard and soft drusen with sizes between 60 and 175 μm exhibited the pattern most clearly (types A and B patterns). In more advanced disease (confluent drusen, around geographic atrophy, near hyperpigmentation), the pattern became less distinct and foci of high and low AF not clearly associated with the loci of drusen were increasingly seen. The monochromatic image of patient 5 (Fig. 4A) showed hard and soft drusen in a patient with AMD. The AF image (Fig. 4B) exhibited numerous foci of low and high AF, some corresponding to drusen but most exhibiting no correspondence to the drusen distribution.

Spatial Correspondence of Drusen and AF Patterns

Image analysis of the AF and monochromatic images of patients 1 to 4 classified the pixels for the entire field in four groups, depending on the presence/absence of low AF pixels in the AF image and the presence/absence of drusen in corresponding pixels of the monochromatic image (Fig. 5). For patients 1 to 4, counts show that the probability of having a low AF over a druse pixel is 0.065, 0.061, 0.040, and 0.073, respectively. The predicted probability of the same event to occur in the case of

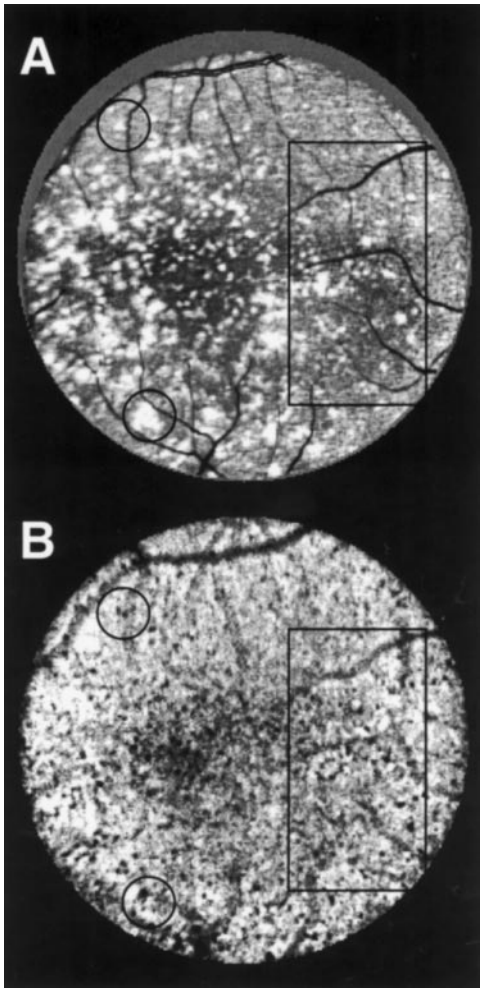

FIGURE 3. Monochromatic (**A**; 550 nm) and autofluorescence (**B**; Ex 550 nm, Em > 590 nm) images in a 69-year-old woman (patient 4) with numerous hard drusen and soft drusen in the macula (right eye; VA, 20/40; fellow eye with a neovascular membrane). Quantitative analysis of individual drusen was performed in the area defined by the *rectangle*.

randomly distributed AF and druse pixels is 0.032, 0.038, 0.020, and 0.040, respectively (dark bars in Fig. 5). Comparison of these probabilities using *Z*-test statistics for each patient separately showed that the null hypothesis, that is, no difference, could be rejected in all cases ($P < 0.001$ for each patient). The observed probabilities were significantly higher than the predicted ones (1.6–2.1 times higher).

AF and Reflectance Distribution over Drusen

The local autofluorescence and reflectance distribution associated with 54 nonconfluent drusen ($n = 17$, 16, 8, and 13 in patients 1, 2, 3, and 4, respectively) were measured in selected areas of the AF and monochromatic images (Figs. 1, 2, 3). Drusen profiles were expressed as relative deviation from the surrounding average backgrounds (Fig. 6); thus, the mean backgrounds were 0, and the SEs associated with those backgrounds were on average 0.012 (range, 0.004–0.021) and 0.007 (range, 0.004–0.010) for the reflectance and AF profiles, respectively.

We observed a continuum of AF profiles (Fig. 6), ranging from those with a distinct annulus of high AF surrounding the low-AF focus (type A) to those without an annulus (type B). If we define type A profiles as having an annulus amplitude $P(r_a)$ larger than $1.96 \cdot \sqrt{2} \cdot$ S.E., then type A profiles were found for 42 of 54 drusen (13/17, 12/16, 8/8, and 9/13 for patients 1, 2, 3, and 4, respectively). Table 1 gives the ranges, means, and correlation with drusen size for the center value $P(0)$, the FWHM, and the dimension and amplitude of the AF annulus.

In this analysis we call "druse size" the FWHM of the reflectance profile (550 nm monochromatic), which is typically 70% ± 18% of the drusen size measured on color transparencies. The FWHM ranged between 40 and 180 μm, with an average of 87 μm. The differences in drusen sizes for types A and B profiles were not statistically significant. The FWHM of the dark center in the AF profile and the diameter of the bright AF annulus were on average 59 and 123 μm, respectively; both measures increase significantly with drusen size. The maximum of the AF annulus corresponded spatially with the edge of the reflectance profile; the maximum AF occurred on average where the reflectance profile fell to 12% ± 17% of its peak

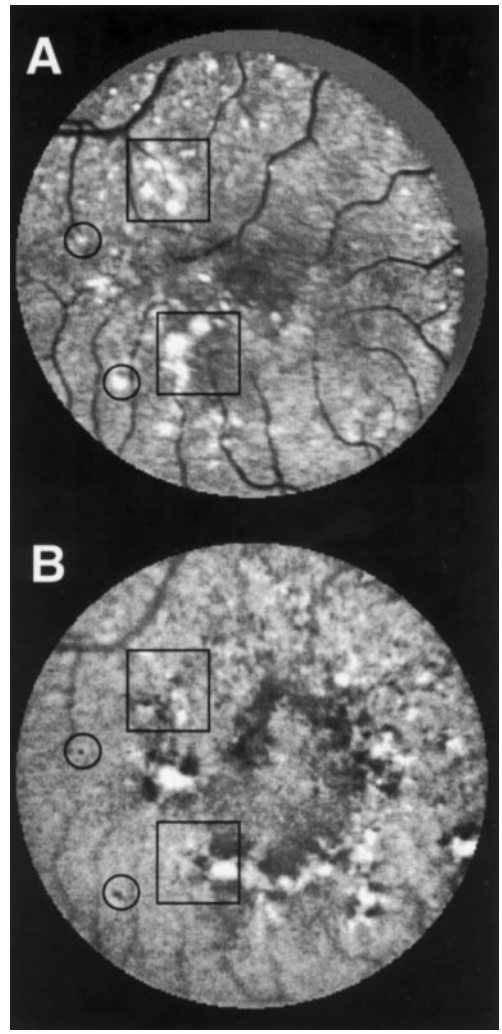

FIGURE 4. Monochromatic (**A**; 550 nm) and autofluorescence (**B**; Ex 550 nm, Em > 590 nm) images in a 80-year-old woman (patient 5) with hard and soft drusen secondary to AMD and impaired central vision (pseudophakic, right eye; VA, 20/60). *Circles* highlight drusen with associated AF pattern, and *squares* indicate areas with heterogeneous AF distribution not corresponding to drusen.

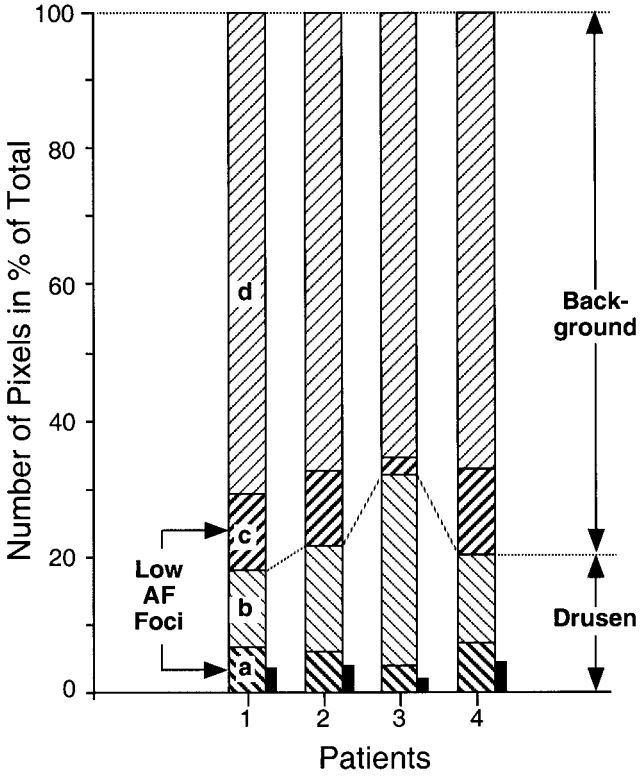

FIGURE 5. Bar graph showing relative pixel counts obtained by image analysis of AF and monochromatic images in patients 1 to 4. Each *bar* is subdivided in 4 groups representing the number of pixels: (a) within a low AF focus and a druse, (b) within a druse but not corresponding to an AF focus, (c) within an AF focus but not corresponding to a druse, and (d) in areas containing neither low AF foci nor drusen. The counts are expressed in percentage of the total number of pixels (24,646, 21,993, 26,769, and 26,544 for patients 1 to 4, respectively). The *dark bar* adjacent group a of each bar represents in percentage of the total the number of pixels that would have correspondingly low AF and drusen if both entities were randomly distributed in their respective images. The observed counts (group a) are significantly higher than the predicted counts.

amplitude. The central spot of the type B profiles were slightly larger ($P = 0.02$) than for type A (68 ± 20 and 56 ± 12 μm, respectively).

The center of the dark AF foci was 3% to 30% less fluorescent than the surrounding AF background (mean, 16%) and the annulus was 2% to 12% more fluorescent than the background (mean, 6%). For the reflectance profile, the drusen center was 9% to 96% more reflecting than the background (mean, 47%). The AF and reflectance center values P(0) were not significantly correlated with drusen size. The central spot of the type B profiles were slightly darker ($P = 0.01$) than for type A (-0.20 ± 0.08 and -0.14 ± 0.07, respectively).

Finally, we compared the center value $P(0)$ of the AF pattern for images obtained with excitation at 470 nm (Fig. 1C) with that for excitation at 550 nm ($n = 29$ drusen, in the 3 patients). As expected from examination of Figures 1C and 1D, the center values were lower with 550-nm than with 470-nm excitation (means, -0.17 ± 0.08 versus -0.08 ± 0.06). The difference was statistically significant (paired *t*-test; $P < 0.0001$), indicating that AF dark foci from the 550-nm image were darker (more negative) and thus more contrasted than those from the 470-nm images.

DISCUSSION

AF imaging is unique because it marks a single layer, the RPE, where the dominant fluorophore, lipofuscin, is located. Areas of RPE atrophy are therefore very clearly delineated.[18–22] The AF is emitted over a large spectral band (500–750 nm) with peak emission at 620 to 640 nm.[15] Although detailed distribution of AF from the RPE can be recorded with our technique, retinal vessels show poor contrast compared to that attained in monochromatic images. This is because only the excitation light is efficiently absorbed by blood, whereas the emitted red fluorescence from the RPE is not (Em > 590 nm for Ex = 550 nm). In addition, the sharpness of the excitation light shadow cast by the vessel on the RPE is degraded by the diffuse nature of the fluorescence emission, causing a reduction in the sharpness of the vessel edges. Retinal vessels have a higher contrast when excited at 470 nm than at 550 nm (Figs. 1B, 1C) because part of the emission spectrum (Em > 515 nm for Ex = 470 nm) is then absorbed by blood.

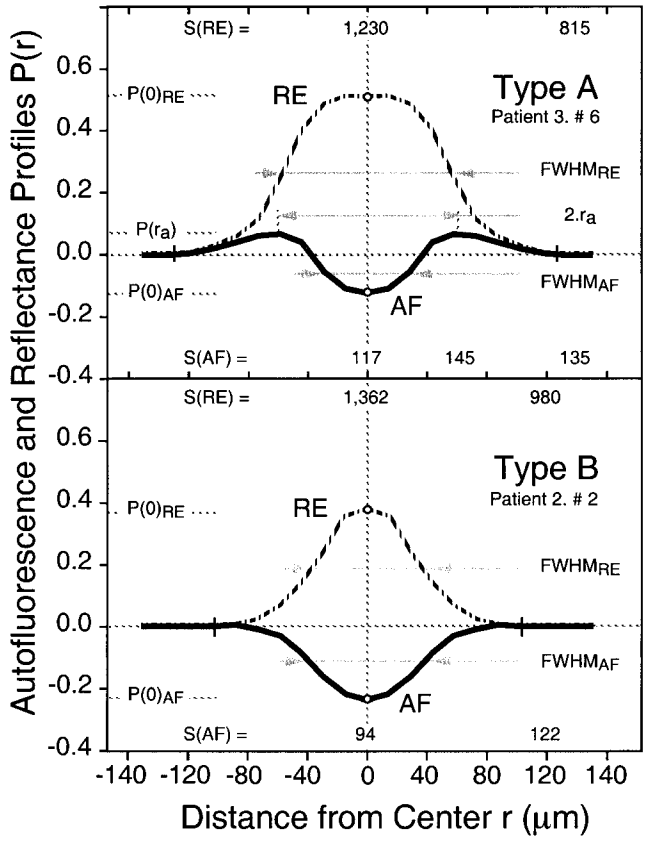

FIGURE 6. Autofluorescence (AF, *solid lines*) and reflectance (RE, *interrupted lines*) distribution at and around two individual drusen (in patients 2 and 3). The ordinate $P(r)$ [see Eq. (1)] is the relative signal deviation from the surrounding background [local signal levels in the original image are indicated by S(RE) and S(AF) for the reflectance and AF profiles, respectively]. Positive (negative) values of $P(r)$ indicate signal levels higher (lower) than the background. Type A autofluorescence profile corresponds with a profile with an annulus of high AF surrounding the central area of low AF. Type B profile has no annulus. The graph shows the profile amplitudes $P(0)$ at the center of the AF and RE profiles, the amplitude $P(r_a)$ and diameter ($2{\cdot}r_a$) of the annulus of high AF, and the full width at half maximum or minimum (FWHM) for each AF and RE profile.

TABLE 1. Characteristics of Autofluorescence Patterns over Drusen

		Range			Correlation with Drusen Size*	
	N	Minimum	Maximum	Mean ± SD	ρ†	*P* Value
Autofluorescence profile						
$FWHM_{AF}$ (μm)	54	32	110	59 ± 15	0.31	0.03
Center minimum $P(0)_{AF}$	54	−0.30	−0.03	−0.16 ± 0.07	0.00	NS
Annulus diameter $2 \cdot r_a$ (μm)	42‡	84	179	123 ± 24	0.66	<0.0001
Annulus $P(r_a)$	42‡	0.015	0.120	0.056 ± 0.028	0.32	0.04
Reflectance profile						
$FWHM_{RE}$ (μm)	54	42	178	87 ± 33	—	—
Center maximum $P(0)_{RE}$	54	0.09	0.96	0.47 ± 0.20	−0.01	NS

See Figure 6 for graphical illustration of the symbols. NS, not significant.

* Drusen size is the FWHM of the reflectance profile.

† Spearmann rank correlation coefficient.

‡ Only type B profiles.

The overall contrast of the AF patterns was found to be higher when using an excitation at 550 nm than at 470 nm. This increase in contrast with excitation wavelength may be explained by the relative increase in the fluorescence of lipofuscin compared to that of drusen. Indeed, lipofuscin and drusen fluorescence with 550-nm excitation are, respectively, higher and lower than with 470-nm excitation.[14,17] The decrease in contrast could also result from a decreased contribution of lens fluorescence either scattered within the lens or reflected by the fundus. The relative contributions of these two components are not known at present but can be expected to show large individual variability; fluorescence reflected by the fundus is likely to be the smallest component.[13] Moreover, with 550-nm excitation light, absorption by ocular media is reduced, and foveal detail is not obscured by macular pigment which absorbs at 470 nm, but not at 550 nm (Figs. 1C, 1D).

In this study, we report a pattern of AF distribution associated with drusen which has not been reported previously. The pattern consists of decreased AF in the center of the druse surrounded, in most cases, by an annulus of increased AF that is spatially correlated with drusen. Moreover, the size of the annulus matches the outer dimension of the druse in the monochromatic images. Although the majority of individual drusen were associated with a pattern, not all foci of low AF were associated with drusen (Fig. 5). It is known that fundus images in AMD reveal only sites of local increases in the diffuse thickening of Bruch's membrane.[4] Infrared imaging of fundi with early AMD reveals drusen and other deposits that are not seen in color and monochromatic imaging.[28]

The dark central focus of the AF pattern is not black, as may be interpreted from examination of the high contrast AF images (Figs. 1, 2, 3) but on average is 16% (and as much as 30%) lower than the surrounding AF background (Table 1). Several factors would tend to increase the signal at the center of the patterns and render them less dark: a contribution of drusen fluorescence would tend to be larger at the drusen center than at its periphery, reflectance of lens fluorescence would also be larger at the center where the drusen reflect most efficiently (Fig. 6), and image degradation of the small dark foci would reduce their contrast. Thus, it is reasonable to expect that the actual distribution of RPE lipofuscin may be more accentuated.

The reduced AF was not due to melanin pigment in the overlying RPE, because the monochromatic images show no evidence of melanin absorption. There are several possible explanations for the observed pattern. (1) RPE stretched over a discrete druse[3,4] may contain a much thinner layer of lipofuscin granules and thus exhibit reduced fluorescence. Cells draped over the sides of a discrete druse may be sampled along longer path lengths (eventually more than one cell), thus creating an annulus of increased fluorescence. This explanation may account for the pattern seen in hard drusen, but is less likely to account for annular patterns of RPE fluorescence over soft drusen, which tend to be flatter thickenings of Bruch's membrane. (2) Another possible explanation for the annular pattern is that the druse causes the central overlying RPE to release lipofuscin granules, which are phagocytosed by RPE at the periphery of the druse, creating reduced central fluorescence surrounded by an annulus of elevated fluorescence. (3) A third possibility is that drusen are formed as a consequence of incipient RPE atrophy. In this model, loss of lysosomal function[12] would lead first to reduced digestion of outer segments membranes and accumulation of lipids in Bruch's membrane.[4] With further erosion of lysosomal capacity, turnover of critical cellular proteins may be so impeded that atrophy follows.

If the annular pattern of AF over drusen represent peripheral displacement of the RPE cells or their granules, with a corresponding thinning from central RPE to peripheral regions, there should be net conservation in the amount of lipofuscin. To test this hypothesis, we calculated the total AF emanating from the entire AF pattern (central dark focus and surrounding annulus) and compared it to the surrounding background. Using the relative profile amplitude $P(r)$ defined in Equation (1), we calculate the total fluorescence AF_{Total} (expressed in μm^2) by integration of the profile:

$$AF_{Total} = 2 \cdot \pi \cdot \sum_{r=0}^{r=r_b} P(r) \cdot r \cdot \Delta r, \quad (2)$$

where r_b is the radius of a circle located just outside the druse. Since $P(r)$ is expressed relative to the background, a resulting value of $AF_{Total} = 0$ would indicate no net difference between

the AF emanating from the druse and the AF emanating in an equivalent area of the surrounding background. In other words (Fig. 5), the increase of AF from the annulus would balance the decreased AF in the central part. We consider that AF_{Total} of a single druse is not different from zero if it is within $\pm 1.96 \cdot \pi r_b^2 \cdot SE$ (SE is the SE associated with the AF background average; see above). For the 54 drusen in 4 patients, AF_{Total} over drusen varied between -2280 and $+2440$ μm^2 (mean, 250 $\pm$ 970 μm^2). AF_{Total} was not significantly different from zero for 41 drusen (35 type A and 6 type B), significantly increased for 7 drusen (all type A), and significantly decreased for 6 drusen (obviously, all type B).

Thus, for most drusen in this small sample, this finding is consistent with a peripheral displacement of the overlying RPE cytoplasm and/or lipofuscin granules without an actual loss of the RPE. However, several drusen had increased total fluorescence, suggesting reduced turnover of lipofuscin and a net increase in the amount of lipofuscin. Alternatively, the fluorescence from the drusen themselves may occasionally be large enough to raise the measured total AF. Finally, and perhaps most importantly, several type B profiles exhibited significant decrease in total AF, which may indicate incipient atrophy of the RPE. These dark AF foci without a distinct annulus were seen in advanced AMD and may mark areas were drusen have regressed. This would be consistent with histopathologic findings that the RPE is attenuated at the site of faded soft drusen.[4]

The AF patterns observed in this study have not been reported by investigators using SLO autofluorescence imaging.[18–22] Although resolution of this apparent discrepancy awaits comparative imaging in the same patients with our technique and the SLO, several reasons for this difference may be identified. As discussed above, the shorter wavelength used in SLO imaging (488 nm) will contribute to a lower contrast for these patterns. The contrast of vessels in SLO images in clearly higher than with our technique, even using the 470-nm excitation. This results from the confocal nature of SLO imaging,[28] where only light from the immediate vicinity of the illuminated image element is sampled, resulting in a reduction of laterally diffused autofluorescent light. Infrared SLO imaging in the indirect mode favors this laterally diffused light and produces images of drusen that have sharp edges, which are sometimes darker than the drusen center.[28,29] These observations cannot be extrapolated to AF imaging because the light emitting layer, the RPE, overlies the drusen. Finally, one cannot rule out that the contrast of SLO imaging—with its low light levels requiring image summation—is inferior to that attainable with our technique.

Hard and soft drusen between 60 and 175 μm in size are characterized by foci of reduced autofluorescence that may or may not be surrounded by an annulus of increased autofluorescence. The formation of larger drusen by fusion of smaller hard or soft drusen is suggested by multiple foci and/or irregular areas of low AF on large drusen. The specific pattern are lost as drusen converge, resulting in the irregular autofluorescence distribution observed for patients with advanced AMD.

Acknowledgments

The authors thank Ann Elsner for valuable suggestions with the data analysis, and Mary–Elisabeth Hartnett and Clement Trempe for helpful discussions concerning this study.

References

1. Bressler NM, Silva JC, Bressler SB, Fine SL, Green WR. Clinicopathologic correlation of drusen and retinal pigment epithelial abnormalities in age-related macular degeneration. *Retina.* 1994;14:130–142.
2. Feeney-Burns L, Ellersieck MR. Age-related changes in the ultrastructure of Bruch's membrane. *Am J Ophthalmol.* 1985;100:686–697.
3. Green WR, Enger C. Age-related macular degeneration histopathologic studies [The 1992 Lorenz E. Zimmerman Lecture]. *Ophthalmology.* 1993;100:1519–1535.
4. Sarks JP, Sarks SH, Killingsworth MC. Evolution of soft drusen in age-related macular degeneration. *Eye.* 1994;8:269–283.
5. Sarks SH, Arnold JJ, Killingsworth MC, Sarks JP. Early drusen formation in the normal and aging eye and their relation to age related maculopathy: a clinical pathological study. *Br J Ophthalmol.* 1999;83:358–368.
6. Holz FG, Sheraidah G, Pauleikhoff D, Bird AC. Analysis of lipid deposits extracted from human macular and peripheral Bruch's membrane. *Arch Ophthamol.* 1994;112:402–406.
7. Feeney–Burns L, Hilderbrand ES, Eldridge S. Aging human RPE: morphometric analysis of macular, equatorial, and peripheral cells. *Invest Ophthalmol Vis Sci.* 1984;25:195–200.
8. Weiter JJ, Delori FC, Wing G, Fitch KA. Retinal pigment epithelial lipofuscin and melanin and choroidal melanin in human eyes. *Invest Ophthalmol Vis Sci.* 1986;27:145–152.
9. Wing GL, Blanchard GC, Weiter JJ. The topography and age relationship of lipofuscin concentration in the retinal pigment epithelium. *Invest Ophthalmol Vis Sci.* 1978;17:601–607.
10. Eldred GE, Katz ML. Fluorophores of the human retinal pigment epithelium: separation and spectral characterization. *Exp Eye Res.* 1988;47:71–86.
11. Reinboth JJ, Gautschi K, Munz K, Eldred GE, Reme CE. Lipofuscin in the retina: quantitative assay for an unprecedented autofluorescent compound (pyridinium bis-retinoid, A2-E) of ocular age pigment. *Exp Eye Res.* 1997;65:639–643.
12. Holz FG, Schutt F, Kopitz J, et al. Inhibition of lysosomal degradative functions in RPE cells by a retinoid component of lipofuscin. *Invest Ophthalmol Vis Sci.* 1999;40:737–743.
13. Delori FC. Spectrophotometer for noninvasive measurement of intrinsic fluorescence and reflectance of the ocular fundus. *Appl Optics.* 1994;33:7439–7452.
14. Delori FC, Arend O, Staurenghi G, Goger D, Dorey CK, Weiter JJ. Lipofuscin and drusen fluorescence in aging and age-related macular degeneration [ARVO Abstract]. *Invest Ophthalmol Vis Sci.* 1994;35(3):**S**2145. Abstract nr 4127.
15. Delori FC, Dorey CK, Staurenghi G, Arend O, Goger DG, Weiter JJ. In vivo fluorescence of the ocular fundus exhibits retinal pigment epithelium lipofuscin characteristics. *Invest Ophthalmol Vis Sci.* 1995;36:718–729.
16. Dorey CK, Staurenghi G, Delori FC. Lipofuscin in aged and AMD eyes. In: Holyfield JG, Anderson RE, La Vail MM, eds. *Retinal Degeneration.* New York: Plenum Press; 1993:3–14.
17. Arend OA, Weiter JJ, Goger DG, Delori FC. In-vivo fundus-fluoreszenz-messungen bei patienten mit alterabhangiger makulardegeneration. *Ophthalmologie.* 1995;92:647–653.
18. von Ruckmann A, Fitzke FW, Bird AC. Distribution of fundus autofluorescence with a scanning laser ophthalmoscope. *Br J Ophthalmol.* 1995;119:543–562.
19. Holz FG, Bellmann C, Margaritidis M, Schutt F, Otto TP, Volcker HE. Patterns of increased in vivo fundus autofluorescence in the junctional zone of geographic atrophy of the retinal pigment epithelium associated with age-related macular degeneration. *Graefes Arch Clin Exp Ophthalmol.* 1999;237:145–52.
20. Solbach U, Keilhauer C, Knabben H, Wolf S. Imaging of retinal autofluorescence in patients with age-related macular degeneration. *Retina.* 1997;17:385–389.
21. Spital G, Radermacher M, Muller C, Brumm G, Lommatzsch A, Pauleikhoff D. Autofluorescence characteristics of lipofuscin com-

ponents in different forms of late senile macular degeneration (German). *Klin Monatsbl Augenheilkd.* 1998;213:23–31 [Ophthalmoscopy Pigment Epithelium of Eye/pathology Prospective Studies 9743935.]

22. von Ruckmann A, Fitzke FW, Bird AC. Fundus autofluorescence in age-related macular disease imaged with a laser scanning ophthalmoscope. *Invest Ophthalmol Vis Sci.* 1997;38:478–486.
23. von Ruckmann A, Schmidt KG, Fitzke FW, Bird AC, Jacobi KW. Dynamics of accumulation and degradation of lipofuscin in retinal pigment epithelium in senile macular degeneration (German). *Klin Monatsbl Augenheilkd.* 1998;213:32–37.
24. Delori FC, Goger DG, Fleckner MR, Burns SA. Multispectral imaging of fundus autofluorescence in normal subjects and AMD patients [ARVO Abstract]. *Invest Ophthalmol Vis Sci.* 1998;39(4): **S**591. Abstract nr 2733.
25. Bird AC, Bressler NM, Bressler SB, et al. An international classification and grading system for age-related maculopathy and agerelated macular degeneration (The International ARM Epidemiological Study Group). *Surv Ophthamol.* 1995;39:367–374.
26. Delori FC, Gragoudas ES, Francisco R, Pruett RC. Monochromatic ophthalmoscopy and fundus photography: the normal fundus. *Arch Ophthalmol.* 1977;95:861–868.
27. ANSI. American National Standard for Safe Use of Lasers. ANSI 136.1-1993 (Revision of ANSI 136.1-1986), 1993.
28. Elsner AE, Burns SA, Weiter JJ, Delori FC. Infrared imaging of sub-retinal structures in the human ocular fundus. *Vision Res.* 1996;36:191–205.
29. Manivannan A, Kirkpatrick JN, Sharp PF, Forrester JV. Clinical investigation of an infrared digital scanning laser ophthalmoscope. *Br J Ophthalmol.* 1994;78:84–90.